Collision Risk Computation accounting for Complex geometries of involved objects

Noelia Sánchez-Ortiz(1), Ignacio Grande-Olalla(1), Klaus Merz(2)

(1) Deimos Space, Ronda de Poniente 19, 28760, Tres Cantos, Madrid, 28760, Spain,
Email: noelia.sanchez@deimos-space.com
(2) ESA/ESOC Space Debris Office (OPS-GR), Robert-Bosch-Str. 5, 64293 Darmstadt, Germany,
Email: Klaus.Merz@esa.int

ABSTRACT

Most of existing algorithms deal with the problem of collision risk assuming spherical objects. This assumption works fine if the size of the satellite is much smaller than the standard deviation of the position uncertainty and it shows approximately the same area for any attitude, as the collision risk will depend on the total area exposed and not to the precise shape of the objects. As the orbit determination algorithms and the surveillance systems improve, this assumption may fail for some satellites. This situation can be solved using complex geometries definition, where a satellite can be defined differently to an sphere.

A method implemented in the ESA operational CORAM tool is presented in this paper. The method is based on addressing complex geometries by assuming a satellite composed of several oriented boxes. The algorithm is based on the computation of the collision volume accounting for the geometry of the two objects. While in the spherical case the hard-body object (collision volume) can be computed as another sphere whose radius is the sum of the radii of the two original spheres, in the complex case this hard body computation is more complicated. It is accomplished by assuming constant attitude and calculating the Minkowski sum of the two objects, and then projecting it onto the encounter plane..

Together with a detailed description of the algorithms, its applicability to some cases is reported, considering different cases of geometries and orbital data accuracy. For spacecraft that cannot be considered as spheres, the consideration of the real geometry of the objects may allow to may allow accepting events which show lower risk than when assessed with the spherical model, or estimate with larger reliability the risk associated to the event. This is of particular importance for the case of large spacecraft as the uncertainty in positions of actual catalogues does not reach small values to make a difference for the case of objects below meter size. As the tracking systems improve and the orbits of catalogued objects are known more precisely, the importance of considering actual shapes of the objects will become more relevant.

Demonstration of feasibility of this algorithm is done through Monte Carlo simulations. The Monte Carlo evaluation of the possible collisions between the two objects, where one of them is at least of complex geometry also require specific considerations summarised along the paper.

These algorithms have been implemented in the ESA operational tool CORAM, developed by Elecnor DEIMOS, which is used for the evaluation of collision risk of ESA operated missions.

1 OVERVIEW

1.1 Collision Risk Computation and Limitations of the Spherical Assumption

Common collision risk algorithms assume the two objects involved in an encounter event are spherical. This assumption allows to easily compute the collision volume projection as the circle of radius equal to the sum of the radii of the two objects. In order to safely evaluate the risk of an encounter with two non-spherical objects, most operators consider the radius of the sphere that includes the complete volume of every object. In this way, it is ensured that any encounter involving the two objects will be identified by evaluating the complete surrounding sphere. The drawback of this approach is that some events reporting large collision risk may not be associated to real high risk events when considering the real shape of the objects (especially for those cases where the objects are very elongated, e.g. having large appendages like solar panels or antennas).

In order to prevent the large number of high risk events raised by the former approach, an equivalent circle can be used for collision risk integration. Such equivalent radius shall be computed to provide the same area as the projected collision volume of the two objects. Then, a method for actually computing the collision volume is

Proc. 7th European Conference on Space Debris, Darmstadt, Germany, 18–21 April 2017, published by the ESA Space Debris Office
Ed. T. Flohrer & F. Schmitz, (http://spacedebris2017.sdo.esoc.esa.int, June 2017)

needed. Additionally, this approach may be appropriate only if the combined covariance is significantly larger than the equivalent radius.

Several authors have proposed algorithms for handling non-spherical objects. [1] proposes the following approach: to obtain the collision cross section of each component and convert it to an equivalent circle having the same area and the same centroid. In [2] Patera provides a method to calculate orbital collision probability without making any simplifying assumptions. A formulation was developed that reduces the two-dimensional integral to a one-dimensional integral involving only a simple exponential function in the integrand. Instead of integrating over an area, the integration can be done along the perimeter of the area, thereby reducing the number of evaluations of the integrand and increasing the computational speed.

1.2 CORAM tool

The algorithm described in this paper has been implemented in the Collision Risk Assessment and Avoidance Manoeuvres (CORAM) tool. The CORAM SW package is intended to support satellite operators in the assessment of conjunction events in regard to the collision risk evaluation and analysis of optimal avoidance manoeuvres. It has been designed to provide large flexibility, by reading the input orbit files in several formats: state vector at an epoch, ephemeris file for an interval, a TLE file or a CDM file; considering different risk evaluation methods, suitable for high and low relative speed encounters and allowing MonteCarlo execution.

Both impulsive and low-thrust manoeuvres can be configured by the operator or added by CORAM during the avoidance manoeuvre optimisation process. The force-model propagator can manage these manoeuvres, both for the state vector and for the covariance matrix, with thruster error modelled as an uncertainty in the acceleration and the direction of the manoeuvre, impacting the evolution of the covariance information.

CORAM is divided in two main different modules.

- CORCOS is the tool responsible for collision risk assessment, input/output of scenario files and propagation.
- CAMOS makes use of CORCOS libraries to compute the optimal avoidance manoeuvre needed by the target satellite to reduce the collision risk (or increase the miss-distance) to a requested level.

The **Collision Risk Computation Software (CORCOS)** is devoted to support the space debris analyst in computing the risk of collision between two objects.

The risk assessment tool allows analysing the probability of collision between orbits with high relative velocity (assumption that allows simplifying the problem and finding simpler algorithms for the probability function) but also for low relative velocities (that in general forces to consider non-linear relative motion, and therefore requires more complex algorithms). As already mentioned, complex geometries (non-spherical objects) are considered (see Fig. 1 for an overview of the main interfaces of CORCOS).

Additionally, the S/W provides all possible conjunctions between two given orbits, inside a predetermined temporal interval, when requested.

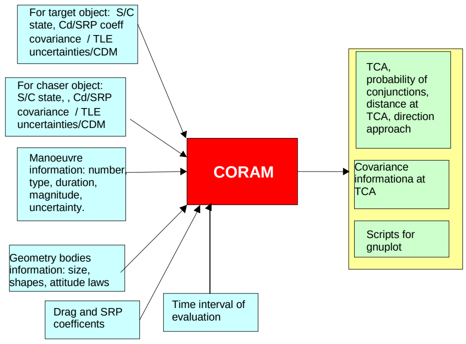

Figure 1.: *Main interfaces of CORCOS*

The **Collision Avoidance Manoeuvre Optimisation Software (CAMOS)** is a tool devoted to the evaluation of different mitigation strategies for the avoidance of a collision risk through the optimisation of avoidance manoeuvres. The tool permits parametric assessments of different avoidance strategies, including the minimisation of a risk function calculated in the loop, or the minimisation of the fuel necessary to attain an acceptable risk level. The tool permits to consider both impulsive and low thrust control and to account for several constraints on the trajectory, as location for GEO satellites or eclipses.

2 ALGORITHM FOR COMPLEX GEOMETRIES

Common collision risk evaluation algorithms deal with the problem of collision risk assuming spherical objects. This assumption may work fine if the size of the satellite is much smaller than the standard deviation of the position uncertainty and it shows approximately the same area for any attitude, as the collision risk will depend on the total area exposed and not to the precise shape of the objects.

As the orbit determination algorithms and the surveillance systems improve, this assumption may fail for some satellites. This situation can be solved using complex geometries definition, where a satellite can be defined by some other parameters than a sphere.

If one of the objects, or both, are complex (composed of oriented boxes), a new method to calculate the collision risk has been devised.

While in the spherical case the hard-body object (collision volume) can be computed as another sphere whose radius is the sum of the radii of the two original spheres, in the complex case this hard body computation is more complicated. It is accomplished by assuming constant attitude and calculating the Minkowski sum of the two objects, and then projecting it onto the encounter plane.. This projection can efficiently treated by projection of the vertices only

2.1 Minkowski Sum

To easily compute the Minkowski sum [3] of two complex objects, it is better to divide the objects in convex shapes and compute the sum by pairs, for all combinations and then reconstruct the final object. The algorithm is based on the computation of the Minkowski sum for every two boxes of the objects but only for the vertex points, without reconstructing or saving any information about the faces. The resulting sum will be also convex.

Those points are then projected onto the encounter plane, and the contour (convex hull) that the points form is calculated. This convex hull is the contour of the projected Minkowski sum, represented as a convex closed irregular polygon. This polygon defines the collision volume, similar to the combined sphere used in the special case. The next step for the developed algorithm is to identify the points in the B-plane that are included within the polygon (shadowed), and those which are outside the polygon.

2.2 Z-buffer Computation

The encounter plane is checked to evaluate which part of it is shadowed by the projected collision volume (complex geometry). This is a problem usually addressed in computer vision programs and games. In the frame of CORAM, it is decided to use the philosophy of the Z-buffer algorithm [4] used in computer vision system within the collision risk frame. Z-buffer refers to the evaluation of the Z value of a 3D object, being Z the direction along the "line of sight" resp. projection direction. In order to compute that, without the aid of graphical representation and visual-tools, the approach considered in this algorithm is based on the evaluation of points in a plane belonging to a polygon. For the sake of the projected area evaluation, the actual Z value is not needed. It is only required to know if the point is shadowed by part of the object.

The encounter plane is discretized and sampled. A z-buffer grid is constructed where every cell of the grid is a true/false indicator of the "shadow" of the hard body onto the encounter plane (See Fig. 2). Every grid cell contains a small amount of contribution of the collision risk and the last step is to compute the risk associated to every shadowed grid cell and sum them up.

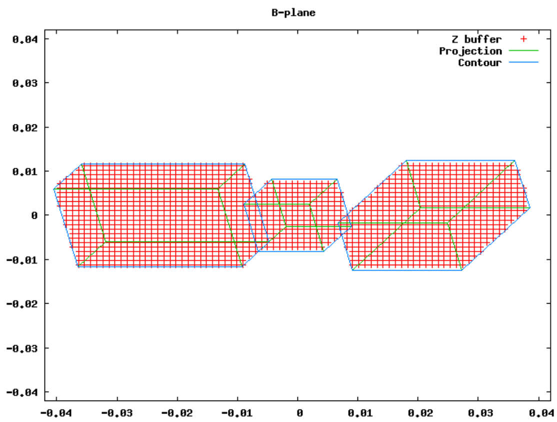

Figure 2. Representation of Encounter plane with the projection of the boxes forming the collision volume the related contour for the case of two satellites and the Z-buffer evaluation.

Only cells not previously shadowed by another already tested polygon are checked by means of a fast *point-in-polygon algorithm*. These steps are repeated for every polygon resulting from a box-box pair of the complex objects, and the resulting z-buffer grid is evaluated to calculate the collision risk. This approach solves the problem of self-shadowing effects and the impact on the evaluated risk.

For the collision risk computation, it is possible to use Alfriend & Akella or Patera methods on each cell. It can be easily done by replacing every cell by an equivalent circle in the encounter plane and applying a collision risk method to them. The final sum provides the total collision risk.

2.3 Evaluation Against Monte Carlo Method

Monte Carlo tests are normally used to evaluate the validity of algorithms. For collision risk evaluation, in the case of spherical objects, it is possible to check for collision by searching the Time of Closest Approach (TCA) by propagating both objects looking for the minimum distance between them, and then checking if the separation distance is lower than the sum of radii.

In the case of geometries made of oriented boxes, however, the simple approach for Monte Carlo followed for the spherical cases is not necessary valid. A suitable algorithm is needed to efficiently implement a Monte Carlo simulation with oriented boxes, which can detect the overlapping of boxes along a period of time around the TCA.

Such algorithm is detailed in [6]. It is based on an algorithm called separating axis test: Two oriented boxes are not separated (i.e. in collision) if, with respect to some axis L, the sum of their projected radii is less than the distance between the projections of their centre points. The separating axis test allows to conclude on absence of collision by testing for collision for a finite number of axes. In the case of two 3-dimensional boxes, it is necessary to check at most 15 of these separating axes to determine if they overlap. These axes correspond to the three coordinate axes of every single box and the nine axes perpendicular to an axis from each. If there is not overlapping in the projection of any of these 15 axes, then there is not overlapping between the two boxes. An example of this test for two dimensions is illustrated in Fig. 3.

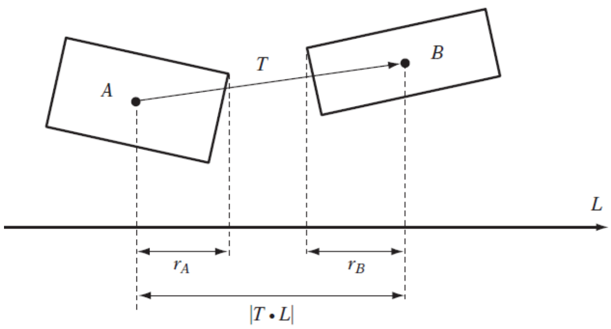

Figure 3. Separating axis test in two dimensions

3 EXAMPLE CASE

This test case demonstrates the capabilities of the developed algorithms for collision risk computation when complex geometries are involved in the event. Different cases of encounters with varying miss-distances, approaching geometries and position uncertainty values are considered.

The event is related to the case of one main object formed by 5 boxes (a main satellite body, two solar panels and two joints between the main body and panels). The second object is a small simple box of 10 cm size. Fig. 4 below provides the encounter configuration of one of the simulated cases.

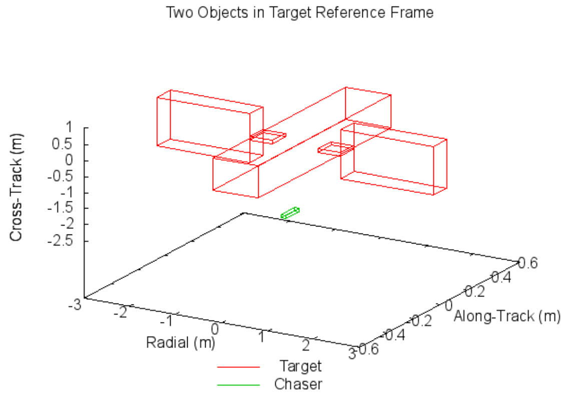

Figure 4. Simulated case for complex geometries. The impact is below the target nominal position.

All the cases have been executed assuming different values of the uncertainty of the two objects' position, resulting in combined accuracy (covariance) at the B-plane of the order of magnitude of 0.2 m 2 m, 20 m and 200 m and separations of 1, 2 and 3 m for the nominal position of the objects.

Each case has been executed with different algorithms: The complex geometry algorithm defined in this paper, the Monte Carlo approach suitable for complex geometries, and the spherical Alfriend and Akella's algorithm [5] for the case of same equivalent projected area in the B-plane.

The simulated case where the nominal encounter point is below the target object does not correspond to an actual collision. When the covariance is very small, this fact can be clearly identified (see Fig. 5). Only the case of miss-distance equal to 1 m offers a relatively high collision risk of 1.9·10-2. For the rest of cases, the density function is almost null over the integration area.

Table 1. Probability Density Function for a test case varying Miss Distance and Combined Position Uncertainty. X direction in the figures below corresponds to Cross Track direction (miss vector direction) in Fig. 4 above.

Position Uncertainty	**Probability Density Function**		
	Miss Distance 1**m**	Miss Distance **2 m**	Miss Distance **3 m**
0.2 m	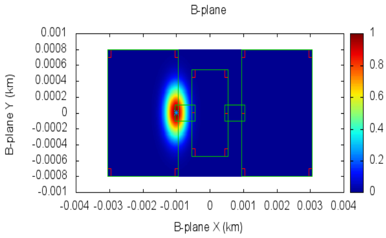	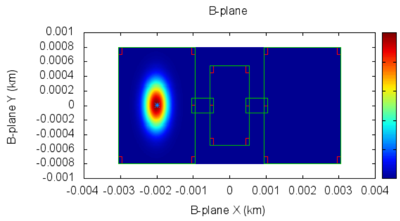	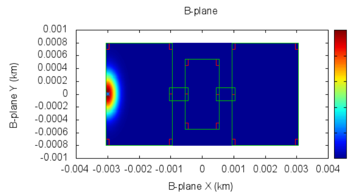
2 m	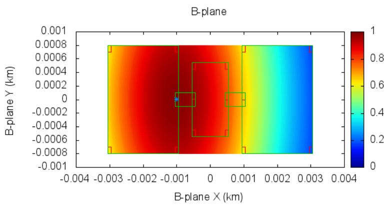	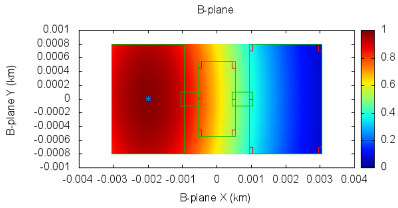	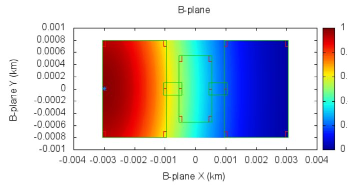
20 m	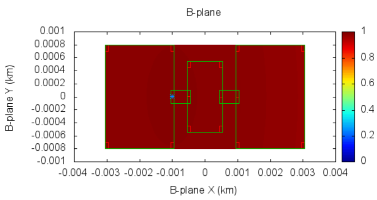	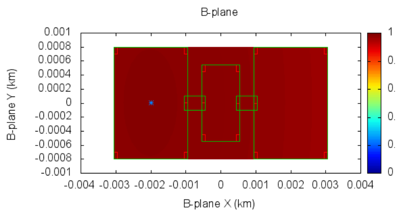	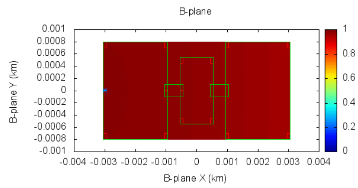

Table 1 provides the probability density function over the B-plane for the analysed cases). For larger uncertainty values, it can be seen that the density function provides significant contribution over the contour surface and thus the collision risk increases when the uncertainty is on the order of magnitude of the miss-distance. For larger uncertainties, the risk is similar for the three simulated miss-distances.

Monte Carlo analysis results are provided below (see Fig. 5), showing a perfect match between the collision probability provided by the Monte Carlo and the probability computed by the algorithm.

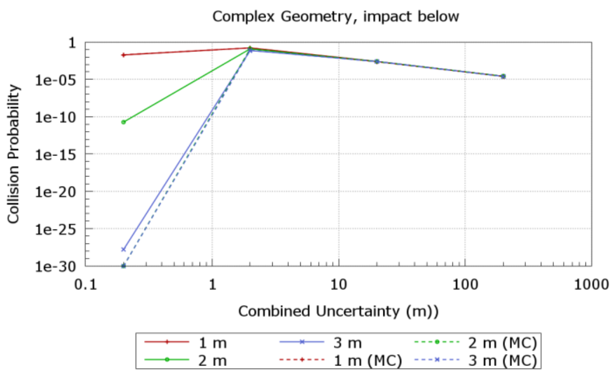

Figure 5. Collision probability for the complex geometries cases (CG algorithm and Monte Carlo comparison), for different miss-distances as a function of the projected covariance value.

Finally, for comparison, risks were computed assuming spherical objects projecting an equivalent area over the B-plane; see Fig. 6 for the results. The equivalent integration area includes the encounter point for the case of miss-distance equal to 1 m, resulting on a wrong large collision probability. For the miss-distance equal to 2 m, the density function still contributes to the equivalent circular integration area, providing larger risk than that computed with the complex geometries algorithm (demonstrated correct thanks to the Monte Carlo executions).

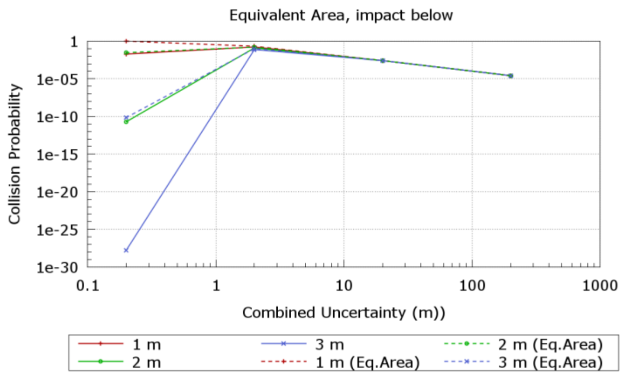

Figure 6. Collision probability for the complex geometries cases (CG algorithm and A&A for Equivalent Area comparison), for different miss-distances as a function of the projected covariance value.

4 THE CASE OF A TETHERED SATELLITE

The complex geometry algorithms are recommended for collision risk computation when the geometry of the involved objects is not similar to that of a sphere. One particular case of interest is that of the tethered satellites. In this type of systems, a very large tether is attached to the main body of a satellite. This creates a complex structure which normally has one dimension much longer than the others. There is a long history of such missions and long tethers up to 20 km length have been used in the past.

In the analysis shown here, the relative dynamics of the tether with respect to the satellite is not considered, and the configured system does not intend to reflect any real case of a tethered system.

The case of a satellite with a 10 km tether is simulated, in order to compute the collision risk for the case of an impact at different miss-distances. The configuration of the main satellite is provided in Fig. 7, with a overall spam of the main satellite of 4 meters and a tether thickness of 20 cm. In the first case shown below, the chaser object impacts the main satellite at the nominal position (miss distance = 0km). A number of additional cases have been simulated, with the miss distance equal to 0, 0.1, 0.5, 1, 10, and 15 km. In all these cases, the chaser object is located in nadir direction from the satellite. Then, for all cases, the chaser impacts the tether attached to the system (except for the case of 15 km miss distance).

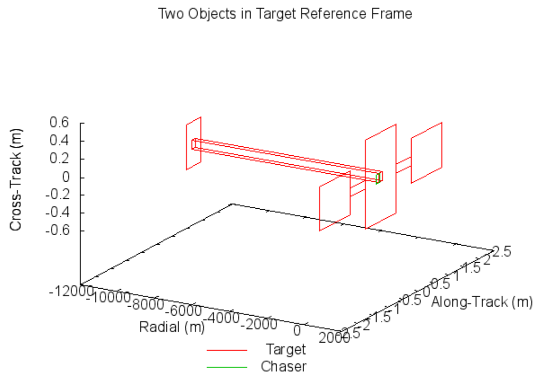

Figure 7. Simulated Satellite for the case of Analysis of Tether case.

All the cases have been executed assuming different values of the uncertainty of the two objects position, resulting in combined accuracy (covariance) at the B-plane of the order of 2 m, 200 m, 2km and 20 km

Each case has been executed using different algorithms. The complex geometry algorithm defined in this paper has been executed for two configurations: the main satellite with the attached tether, and the main satellite without the tether. Additionally, the simple Alfriend&Akella's method for spherical objects has been executed. In this case, the configuration is chosen so the equivalent diameter of the cross-section in the B-plane is equal to the one resulting from the tether case. This resulting diameter is 49 m.

From next Fig. 8, where the complete tethered system is considered, the probability evolves similarly for all the analyzed miss-distances (between nominal center of the main satellite and the chaser) but for the case where the theoretical impact occurs out of the tether nominal position (15 km miss-distance). As the chaser object impacts the tether system, when applying the algorithm for complex geometries, similar collision probabilities are obtained for all the different distance values between nominal positions when the same uncertainty is considered. The probability diminishes for all cases as the uncertainty increases, as the chances that the chaser impacts the nominal position reduce when increasing the uncertainty of those nominal positions. The case of a 15 km miss-distance, which is not a real encounter (conjunction leading in an actual hit), provides null probability for combined uncertainties in the B-Plane around 200 m and below. For larger uncertainties, a non-zero probability results, being this risk similar to the other miss distance cases.

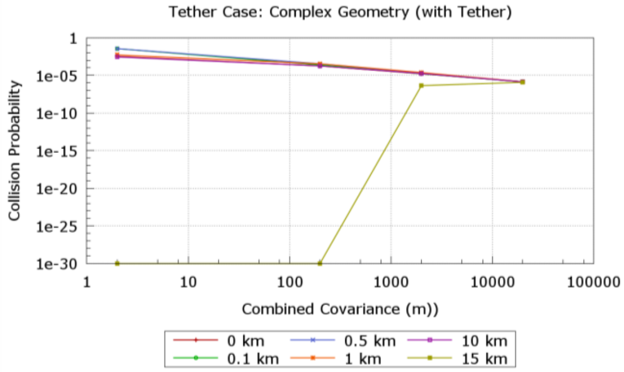

Figure 8. Collision probability for the Tethered Satellite, for different miss-distances as a function of the projected covariance value.

If the tether system is not considered for evaluation of collision risk, the resulting probabilities are similar to those of the former case for the miss-distance equal to zero. For the other cases, and when the position uncertainty is small, the collision probability is very low, as it is only evaluated over the main satellite, and not over the tether (where the actual collision occurs). When the uncertainty is large (larger than the miss-distance) the collision probability is similar among all the cases. Still, the collision probability is below that from the complete tethered system. This fact demonstrates that the complete system shall be considered for reliable computation of collision risk in those tethered satellite systems.

The complex geometry case with the complete tethered system provides an equivalent projected area of 49 m span over the collision B-plane. Considering this diameter, and applying the spherical case algorithm defined by Alfrend&Akella, the resulting collision probability is only close to the actual risk for the case of very small miss-distance or for the case of large uncertainties (where the integral of the density function over the equivalent area result in similar probability than integrating over the actual area). To obtain realistic risk figures using this spherical model, it is needed that the miss distance is on the order of magnitude of the uncertainty value.

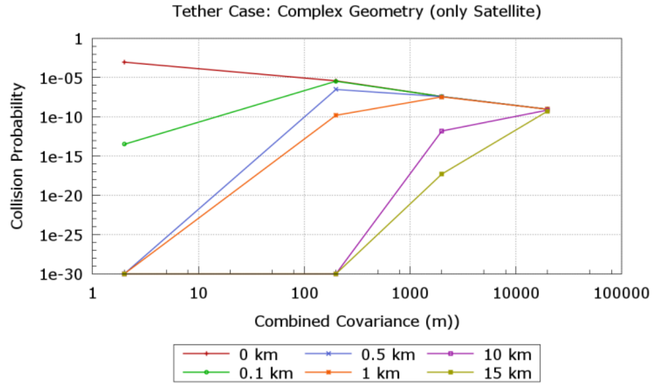

Figure 9. Collision probability for the Main Satellite, for different miss-distances as a function of the projected covariance value.

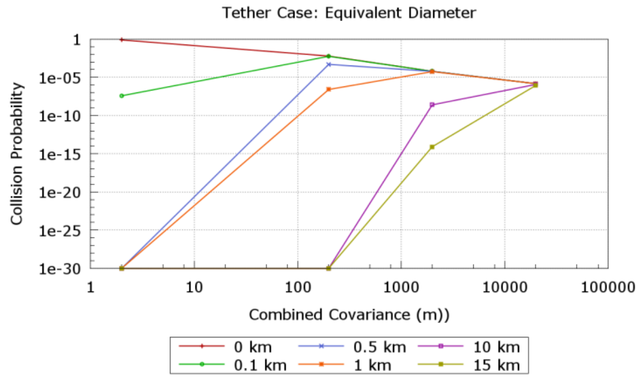

Figure 10. Collision probability for the Equivalent Sphere than the Tethered system, for different miss-distances as a function of the projected covariance value.

In order to evaluate the risk by A&A algorithm as above, it is needed to know the projected area over the B-plane. For that, the Z-buffer algorithm presented above has been used. Even for those cases, with large uncertainties, where the spherical assumption may be acceptable, the developed algorithm is useful for the computation of such projected area.

In the case the projected area cannot be computed, and for the safest configuration. All conjunctions over the sphere including the complete system should be considered. This would correspond to an enormous 20 km diameter sphere, resulting on a non-reliable collision risk computation approach. For those cases, it would be needed to estimate, instead of the collision risk, the miss-distance, and only in case of having an impact in the nadir direction; it would be required to analyze it further. This option is not recommended, especially due to the performances of the developed algorithm and the simplicity of its implementation.

In the following, each miss distance case is shown for the three executed approaches. It can be observed that for the miss distance equal to 0, the collision risk reported by the complex geometry case does not reach 1. This is caused by the density function to be spread over a longer area than that used for integration.

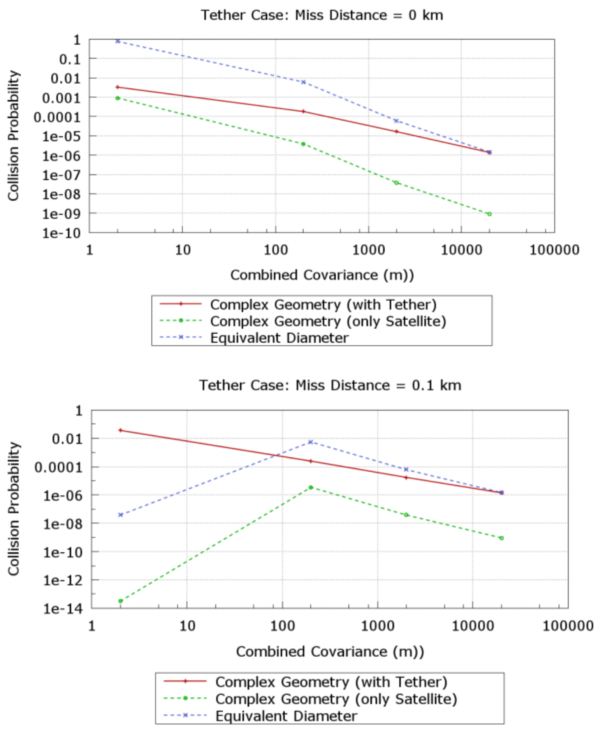

Figure 11. Collision probability for tether system with different collision risk computation approaches, for different miss-distances (0 and 0.1 km) as a function of the projected covariance value.

It can be easily observed that the collision probability when considering only the main satellite (without the tether) is well below the collision risk of the complete system. Only in the case of the chaser nominally impacting the main satellite, this approach would result in adequate probabilities for the very accurate covariance cases (on the order of meters). For more realistic cases (over 20 m), the results with this approach are not considered reliable.

The case of equivalent area used for a simple algorithm is suitable when the position uncertainty values are large. It can be observed that, the larger the miss-distance is, the larger the position uncertainty is needed to get a collision probability equivalent to that from the complex approach. Additionally, as it has already been mentioned, this approach requires a method to compute the projected area allowing to derive the equivalent sphere diameter, for which the developed Z-buffer algorithm can be considered.

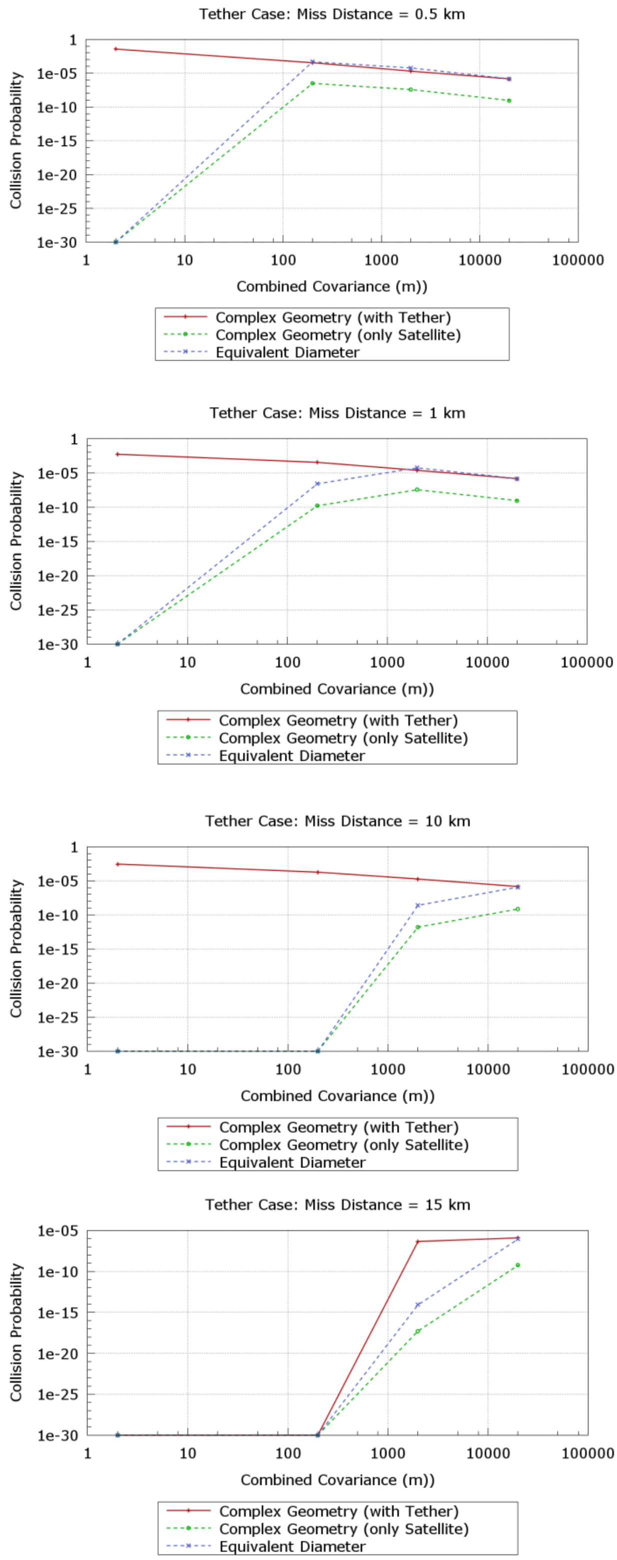

Figure 12. Collision probability for tether system with different collision risk computation approaches, for different miss-distances (0.5, 1, 10 and 15 km) as a function of the projected covariance value.

If we consider now a conjunction with nominal encounter which does not impact exactly at the tether, but 100 meters apart, we see that the collision risk evaluation is more useful than simple distance evaluation: For two scenarios of a close approach at 100 resp. 500 m distance from the main object along the tether direction two cases each are considered, one nominally impacting the tether, i.e. 0 distance to the tether, and the other one having a miss-distance of 100 m, perpendicular to the tether direction (additional to the 100 resp. 500 m separation from the main body). The combined uncertainty in the B-plane is 200m.

Table 2. Comparison of Conjunction cases for a tethered satellite

Distance to Main Satellite (along tether direction)	Distance to Main Satellite (perpendicular to tether direction)	Collision Probability with Main Satellite Only	Collision Probability with Satellite plus Tether
100 m	0 m	$3.4\cdot10^{-6}$	$2.43\cdot10^{-4}$
100 m	100 m	$3.12\cdot10^{-6}$	$2.18\cdot10^{-4}$
500 m	0 m	$3.07\cdot10^{-7}$	$3.48\cdot10^{-4}$
500 m	100 m	$2.82\cdot10^{-7}$	$6.08\cdot10^{-5}$

For the scenario of a miss-distance of 100 m along the tether direction from the main-body the two cases of nominally hitting the tether or passing by 100 m perpendicular to it show similar risks. As the uncertainty is on the level of the miss-distance perpendicular to tether, there is a significant part of the risk integrated over the collision area for both cases. Additionally, the probability density function over the main satellite is also similar. In this particular case, it can be seen that, typically used collision probability thresholds (between 10^{-5} and 10^{-4}) would force on an avoidance manoeuvre for the case of considering the tether when integrating the risk (using complex geometries algorithms).

In the case of 0.5 km distance to the main satellite along the tether direction, for both cases (miss-distance perpendicular to the tether direction 0 or 100 m) the collision risk when considering only the satellite is very small, in spite of having a significant risk to collide with the tether. When considering the complex system composed by main satellite and tether, the estimated risk reaches levels in the range which usually trigger an avoidance manoeuvre.

5 CONCLUSIONS

Most of the existing algorithms dealing with the problem of collision risk assume spherical objects. This assumption works fine if the size of the satellite is much smaller than the standard deviation of the position uncertainty and it shows approximately the same area for any attitude, as the collision risk will depend on the total area exposed and not to the precise shape of the objects.

A new method that allows the consideration of complex geometries is presented in this paper and its applicability to a very elongated spacecraft is reported. Demonstration of feasibility of this algorithm is done through Monte Carlo simulations.

From the presented cases, it can be seen that an algorithm accounting for the actual shape of the colliding objects may allow accepting (i.e. not performing an avoidance manoeuvre) conjunctions which would show a high risk assuming spherical shape. This is particularly the case if the uncertainty associated to the objects' positions is below the order of magnitude of the conjunction miss distance and the size of the object in some direction.

The use of appropriate collision risk algorithms accounting for objects geometry is of particular importance for the case of large spacecraft as the uncertainty in positions of actual catalogues does not reach small values to make a difference for the case of objects below meter size. As the tracking systems improve and the orbits of catalogued objects are known more precisely, the importance of considering actual shapes of the objects will become more relevant.

6 REFERENCES

1. Chan, K., "Short-term vs long-term spacecraft encounters", AIAA Paper, No.2004-5460.
2. Patera, R. General Method for Calculating Satellite Collision Probability. Journal of Guidance, Control & Dynamics, vol.24:716-722, Jul./Aug. 2001
3. http://en.wikipedia.org/ wiki/ Minkowski_addition. Checked on 21-04-2013.
4. http://en.wikipedia.org/wiki/Z-buffering. Checked on 21-04-2013.
5. M.R. Akella, K.T. Alfriend. (2000) "*Probability of collision between space objects*", Journal of Guidance, Control and Dynamics, Vol.23, No.5, pp.769-772.
6. Ericson, Christer. "Real-time collision detection", Elsevier.